Solid State Sciences 127 (2022) 106861

Contents lists available at ScienceDirect

Solid State Sciences

journal homepage: www.elsevier.com/locate/ssscie

Synthesis, structure, and scintillation of $Rb_4Ta_2Si_8O_{23}$

Darren Carone [a], Luiz G. Jacobsohn [b], Logan S. Breton [a], Hans-Conrad zur Loye [a,*]

[a] Department of Chemistry and Biochemistry, University of South Carolina, Columbia, SC, 29208, USA
[b] Department of Materials Science and Engineering, Clemson University, Clemson, SC, 29634, USA

ARTICLE INFO

Keywords:
Flux crystal growth
Crystal structure
Photoluminescence
Scintillation

ABSTRACT

A new tantalum silicate, $Rb_4Ta_2Si_8O_{23}$, was synthesized as high-quality single crystals by the high temperature flux growth method. $Rb_4Ta_2Si_8O_{23}$ was found to exhibit intense blue luminescence and scintillation as a self-activated luminescent silicate. $Rb_4Ta_2Si_8O_{23}$ crystallizes in the triclinic space group $P\bar{1}$ with lattice parameters of $a = 6.8916(2)$ Å, $b = 7.7669(2)$ Å, $c = 11.0018(3)$ Å, $\alpha = 76.3110(10)°$, $\beta = 89.2560(10)°$, and $\gamma = 71.8090(10)°$. The structure consists of corner-sharing SiO_4 tetrahedra forming infinite ribbons connected by isolated TaO_6 octahedra. The synthesis, structure, and optical properties are reported, notably, bright blue scintillation when exposed to X-rays. The scintillation of $Rb_4Ta_2Si_8O_{23}$ was quantitatively evaluated by radioluminescence (RL) measurements and was determined to be ~47% of BGO powder.

1. Introduction

Scintillators are materials that absorb high-energy ionizing radiation, such as X-rays and gamma-rays, and create electron hole pairs. Scintillation is observed when these excited electrons return to the ground state via a radiative process. Scintillators are widely used in numerous applications, including X-ray phosphors, positron emission tomography (PET) [1], computer tomography (CT) scanners [2], X-ray and neutron detectors, and nuclear detection systems by homeland security. Many of the currently used inorganic scintillators include the doped inorganic halides NaI:Tl [3], CsI:Tl [4], Cs_2LiYCl_6:Ce [5], covalent oxides, such as $Lu_2SiO_5:Ce^{3+}$ [6], $Lu_3Al_5O_{12}:Ce^{3+}$ [7], and self-activated oxides, such as $CdWO_4$ [8] and $Bi_4Ge_3O_{12}$ (BGO) [9]. Ideal characteristics of an ideal scintillator, which are application specific, include a high light yield, a fast response time, moisture inertness, and stability at high temperatures. The wide variety of uses for scintillators requiring specialized features lead to the continued interest in the development of new materials with optimized scintillation behavior.

One strategy for the discovery of new scintillators with increased performance is based on the incorporation of certain lanthanides, Ce^{3+} being the most used activator, due to their high atomic number and the ease at which their excited states become populated coupled with their likelihood to follow a radiative decay back to the ground state. Although a valid strategy, the recent increase in the cost of rare earth elements has motivated the search for new scintillation materials that do not require the presence of rare earth luminescent centers. A promising alternative to rare earth activated phosphors are broad classes of luminescent oxides that are self-activated i.e., intrinsically luminescent. Self-activated luminescent oxides are comprised of a host lattice typically containing metals having a d^0 electronic configuration, mainly early-transition metals such as Nb^{5+} or Ta^{5+}, which can exhibit intense luminescence and scintillation, $MgWO_4$ being a well-known example.

The crystal growth of new luminescent and scintillating materials via mild hydrothermal and high temperature flux growth methods has long been used as an efficient synthetic strategy that has led to the discovery of a large number of such materials [10–13], notably, intensely scintillating rare-earth activated mixed anion silicates $Cs_3RESi_4O_{10}F_2$ (RE = Y, Eu – Lu) [14], and the self-activated oxyfluoride scintillators $BaWO_2F_4$ [15] and $Cs_{10}(Nb_2O_2F_9)_3F$ [16]. These discoveries have motivated us to further explore these classes of scintillator materials, in particular, those based on silicate and germanate host structures, either rare-earth or self-activated, due to their optimal band gap energies and their ability to form diverse framework structures capable of incorporating a variety of luminescent centers.

Herein, we report a new tantalum silicate of the composition $Rb_4Ta_2Si_8O_{23}$ grown as single crystals from a high temperature RbCl/RbF flux. This material exhibits broad blue emission under UV-light excitation at room temperature. Furthermore, $Rb_4Ta_2Si_8O_{23}$ was found to scintillate and emit intense blue light when exposed to laboratory X-rays. The scintillation of $Rb_4Ta_2Si_8O_{23}$ was studied by radioluminescence (RL) measurements, which revealed sustained scintillation intensity at 300 °C and, quantitatively, integral RL emission of

* Corresponding author.
E-mail address: zurloye@mailbox.sc.edu (H.-C. zur Loye).

https://doi.org/10.1016/j.solidstatesciences.2022.106861
Received 1 March 2022; Accepted 15 March 2022
Available online 23 March 2022

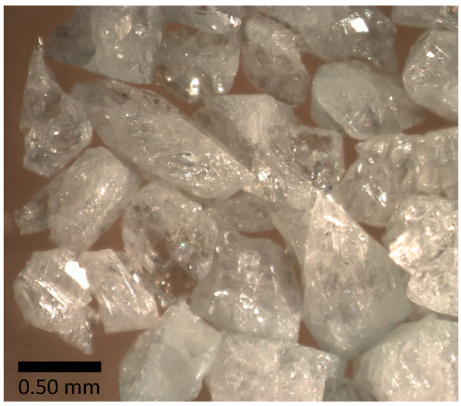

Fig. 1. Optical microscopy image showing representative crystals of $Rb_4Ta_2Si_8O_{23}$.

Table 1
Crystallographic and refinement data for $Rb_4Ta_2Si_8O_{23}$.

Chemical formula	$O_{23}Rb_4Si_8Ta_2$
Formula weight	1296.50
Crystal system	Triclinic
Space group, Z	$P\bar{1}$, 2
a, Å	6.8916(2)
b, Å	7.7669(2)
c, Å^3	11.0018(3)
α, deg	76.3110(10)
β, deg	89.2560(10)
γ, deg	71.8090(10)
ρ_{calcd}, g/cm^3	3.969
Radiation (λ, Å)	MoK_α (0.71073)
μ, mm^{-1}	19.549
T, K	299(2)
Crystal dim., mm^3	0.07 × 0.04 x 0.03
2θ range, deg.	2.847–29.998
Reflections collected	41821
Data/parameters/restraints	3134/170/0
R_{int}	0.0362
Goodness of fit	1.241
Final R indices [I > 2sigma(I)]	$R_1 = 0.0112$ w$R_2 = 0.0287$
R indices (all data)	$R_1 = 0.0113$ w$R_2 = 0.0288$
Largest diff. peak and hole	0.845 and −0.646 e.Å^{-3}

approximately 47% of BGO powder at room temperature.

2. Experimental

2.1. Reagents

Ta_2O_5 (Alfa Aesar, 99%), SiO_2 (Alfa Aesar, 99.9%), and RbCl (Alfa Aesar, 99.8%) were used as received. RbF (Strem, 99.8%) was also used as received, although found to be $HRbF_2$ by powder X-ray diffraction analysis.

2.1.1. Crystal growth

Single crystals of $Rb_4Ta_2Si_8O_{23}$ were grown from a mixed alkali halide eutectic flux. A cylindrical silver crucible (1.2 cm D x 5.7 cm H) was charged with 0.5 mmol Ta_2O_5, 2 mmol of SiO_2, and a mixture of 14 mmol of RbCl and 12.5 mmol of RbF. The reaction mixture was quickly heated to 900 °C, held there for 12 h, slow cooled to 450 °C at a rate of 6 °C/h, and finally cooled to room temperature by turning off the furnace. The solidified flux was dissolved in water, aided by sonication, and the crystals were isolated by vacuum filtration. $Rb_4Ta_2Si_8O_{23}$ was obtained as colorless, irregularly shaped crystals (Fig. 1) nearing 1 mm^3 in size, along with AgCl powder, which was removed using a concentrated sodium thiosulfate solution. Large crystals of $Rb_4Ta_2Si_8O_{23}$ were hand-picked for property measurements.

2.2. Single-crystal X-ray diffraction

X-ray diffraction intensity data were collected on a shard cut from a large single crystal of $Rb_4Ta_2Si_8O_{23}$ at 299(2) K using a Bruker D8 Quest diffractometer equipped with a PHOTON 100 CMOS area detector and an Incoatec microfocus source (Mo Kα radiation, λ = 0.71073 Å). The crystal was mounted on a microloop using immersion oil. The raw data reduction and absorption corrections were performed using SAINT+ and SADABS programs [17,18]. An initial structure solution was obtained with SHELXS-2017 using direct methods and Olex2 GUI [19]. Full-matrix least-square refinements against F^2 were performed with SHELXL software [20]. The structure was checked for missing symmetry with the Addsym program implemented within PLATON software and no higher symmetry was found [21]. The crystallographic data are summarized in Table 1.

2.3. Powder X-ray diffraction

Powder X-ray diffraction data were collected on a Bruker D2 Phaser powder X-ray diffractometer using Cu Kα radiation. The step scan covered the angular range 5–65° 2θ in steps of 0.04°. An overlaid experimental and calculated PXRD pattern for $Rb_4Ta_2Si_8O_{23}$ is provided as Figure S1.

2.4. Optical properties

The photoluminescence spectrum was collected on a powdered sample of $Rb_4Ta_2Si_8O_{23}$ at room temperature using a PerkinElmer LS 55 fluorescence spectrometer. Emission scans were performed in the 300–800 nm range with an excitation wavelength of 254 nm.

2.4.1. Scintillation

Radioluminescence (RL) measurements were taken using a customer-designed configuration of the Freiberg Instruments Lexsyg spectrofluorometer equipped with a Varian Medical Systems VF-50J X-ray tube with a tungsten target. The X-ray source was coupled with a Crystal Photonics CXD-S10 photodiode for continuous radiation intensity monitoring. The light emitted by the sample was collected by an Andor Technology SR-OPT-8024 optical fiber connected to an Andor Technology Shamrock 163 spectograph coupled to a cooled (−80 °C) Andor Technology DU920P-BU Newton CCD camera (spectral resolution of ~0.5 nm/pixel). A powdered sample filled a ~8 mm diameter, 0.5 mm deep cup, thus allowing for relative RL intensity with bismuth germanium oxide (BGO) powder (Alfa Aesar Puratronic, 99.9995% (metals basis)) used as a reference. RL was measured under continuous X-ray irradiation (40 kV, 1 mA) with an integration time of 1 s. RL measurements as a function of temperature were executed under continuous heating with a 0.5 °C/s heating rate up to 500 °C and a 4 s integration time. Thus, temperature increased by 2 °C during the acquisition of each spectrum. Spectra were labeled by the starting acquisition temperature. Spectra were automatically corrected using the spectral response of the system determined by the manufacturer.

Scintillation images of $Rb_4Ta_2Si_8O_{23}$ single crystals were taken using a digital camera inside a Rigaku Ultima IV diffractometer equipped with a Cu Kα source (λ = 1.54018 Å).

3. Results and discussion

3.1. Crystal structure

$Rb_4Ta_2Si_8O_{23}$ crystallizes in the triclinic space group $P\bar{1}$ with lattice parameters of $a = 6.8916(2)$ Å, $b = 7.7669(2)$ Å, $c = 11.0018(3)$ Å, $\alpha = 76.3110(10)°$, $\beta = 89.2560(10)°$, and $\gamma = 71.8090(10)°$. The structure is

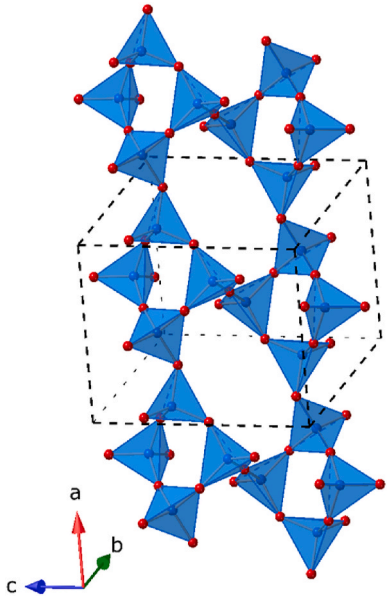

Fig. 2. Ribbons of corner-sharing SiO_4 tetrahedra which make up Si_4O_{12} units running along the a-axis.

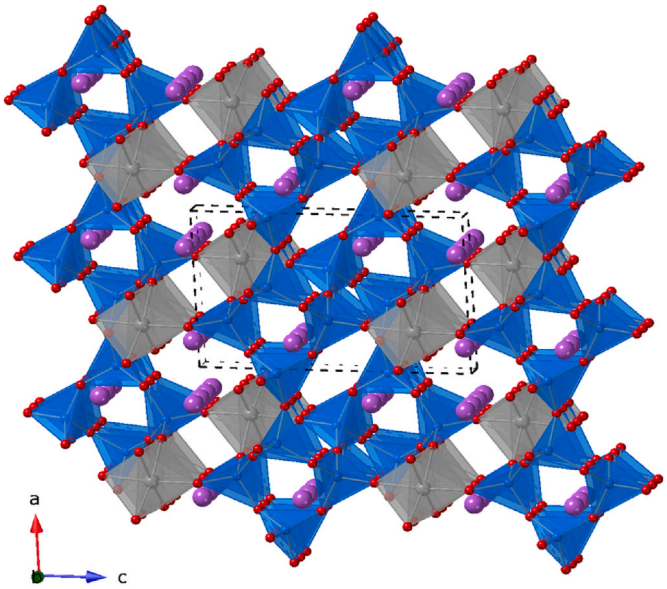

Fig. 3. Overall structure of $Rb_4Ta_2Si_8O_{23}$ viewed along the *b*-axis. TaO_6 octahedra are shown in grey, SiO_4 tetrahedra in blue, Rb atoms in purple, and O atoms in red. (For interpretation of the references to color in this figure legend, the reader is referred to the Web version of this article.)

analogous to previous reports on $Rb_4(NbO)_2(Si_8O_{21})$ and $Cs_4(NbO)_2(Si_8O_{21})$ by Kao et al. and Crosnier et al. respectively [22,23]. The structure of $Rb_4Ta_2Si_8O_{23}$ can best be described as a ribbon-based silicate consisting of SiO_4 tetrahedra that are corner-sharing to create Si_4O_{12} units, which make up the ribbons running along the *a*-axis (Fig. 2).

There are four crystallographically unique silicon positions with Si—O bond lengths ranging from 1.5643(16) to 1.6329(15) Å. The ribbons of SiO_4 tetrahedra are connected by TaO_6 octahedra to form the overall 3D framework structure (Fig. 3). There is one unique tantalum position; tantalum is coordinated to six oxygen atoms with bond lengths ranging from 1.7740(15) to 2.0257(14) Å, with five of the six oxygens sharing corners with the silicon tetrahedra of the ribbons. The resultant framework contains cavities occupied by the Rb cations for charge balance.

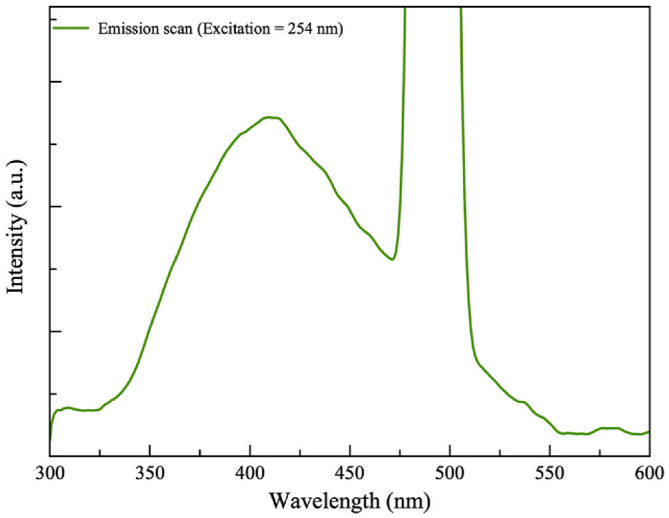

Fig. 4. Emission spectrum for $Rb_4Ta_2Si_8O_{23}$. Intense signal at approximately 500 nm is a 2nd order scattering artifact of the excitation light.

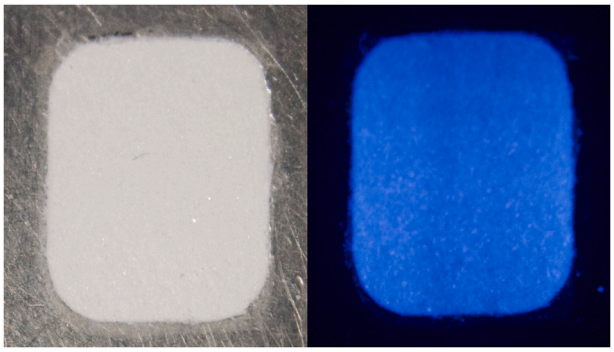

Fig. 5. Optical image of (left) $Rb_4Ta_2Si_8O_{23}$ in the absence of X-rays and (right) $Rb_4Ta_2Si_8O_{23}$ under X-ray excitation.

Optical Properties

Crystals of $Rb_4Ta_2Si_8O_{23}$ were found to luminesce intensely under short-wave UV light exposure. The emission spectrum under 254 nm excitation is shown in Fig. 4, consisting of one broad emission band centered at approximately 409 nm. This broad fluorescence in the UV to blue region is consistent with the deep blue color observed in the luminescent crystals. Blasse et al. also observed significant room temperature luminescence in the niobium silicates $Rb_4(NbO)_2(Si_8O_{21})$ and $Cs_4(NbO)_2(Si_8O_{21})$ with an emission maximum at 470 nm [24].

With strong fluorescence being observed, a primary requirement for a material to exhibit scintillation, a powdered sample of $Rb_4Ta_2Si_8O_{23}$ was irradiated by X-rays to check for emission. $Rb_4Ta_2Si_8O_{23}$ was further found to scintillate intensely as a nice blue color and was captured optically (Fig. 5). The scintillation response of $Rb_4Ta_2Si_8O_{23}$ in powder form was investigated under X-ray radiation through RL measurements. Fig. 6a shows the RL spectra of $Rb_4Ta_2Si_8O_{23}$ measured between room temperature and incrementally up to 500 °C. Similarly, to the photoluminescence spectrum, one broad emission band is observed, this time centered at approximately 422 nm. As a quantitative measure, the integral RL emission between 300 and 750 nm of $Rb_4Ta_2Si_8O_{23}$ was ~47% of BGO powder at room temperature. As expected, due to thermal quenching the increase of temperature leads to a steady decrease of the peak intensity. However, this decrease in peak intensity was observed to

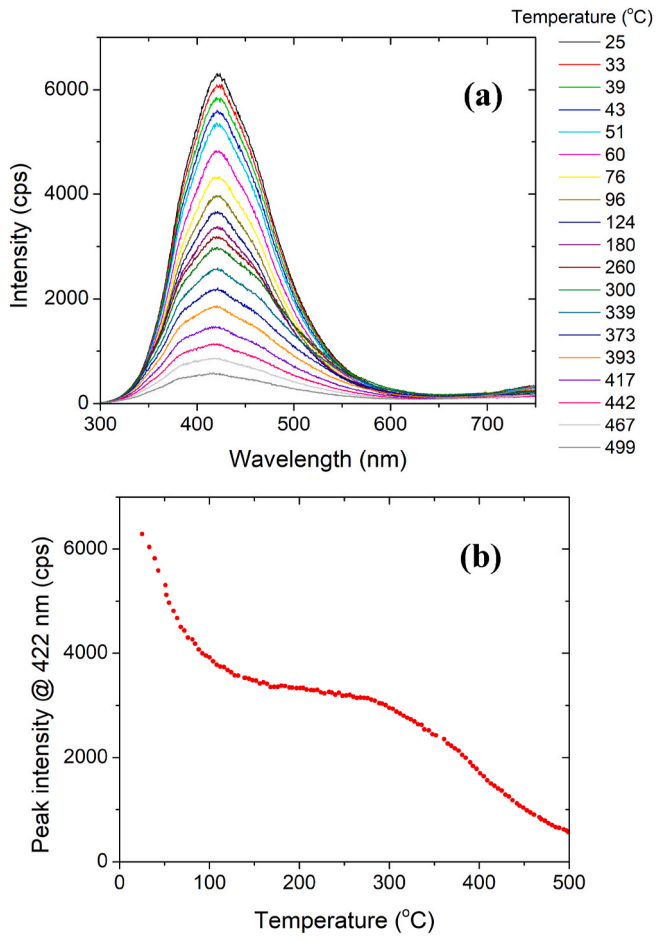

Fig. 6. (a) Selected RL spectra of $Rb_4Ta_2Si_8O_{23}$ up to 500 °C. The weak intensity observed above 700 nm for higher temperatures is originated from the blackbody radiation of the instrument. (b) Peak intensity at 422 nm as a function of temperature.

slow down and stabilize between about 100 and 300 °C. In this temperature range, we observed approximately 50% of the peak intensity was maintained. This is clearly seen in a plot of peak intensity at 422 nm as a function of temperature (Fig. 6b).

Conclusion

A new tantalum silicate X-ray scintillator, $Rb_4Ta_2Si_8O_{23}$, was synthesized by high temperature flux growth as high-quality single crystals grown from a RbCl/RbF flux. The structure consists of infinite ribbons of SiO_4 tetrahedra connected by TaO_6 octahedra to form a 3D framework. $Rb_4Ta_2Si_8O_{23}$ was found to luminescence intensely under short-wave UV light and, furthermore, scintillates intensely under exposure to X-rays. Radioluminescence measurements revealed a resistance to thermal quenching of the scintillation response up to 500 °C and quantitative emission was determined to be ~47% of BGO powder at room temperature.

Accession Codes

CCDC 2154592 contain the supplementary crystallographic data for this paper. These data can be obtained free of charge via www.ccdc.cam.ac.uk/data_request/cif, or by emailing data_request@ccdc.cam.ac.uk, or by contacting The Cambridge Crystallographic Data Centre, 12 Union Road, Cambridge CB2 1EZ, UK; fax: +44 1223 336033.

Declaration of competing interest

The authors declare that they have no known competing financial interests or personal relationships that could have appeared to influence the work reported in this paper.

Acknowledgements

Financial support for this work provided by the National Science Foundation under DMR-1806279 and DMR-1653016 is gratefully acknowledged. Syntheses, structure determination, photoluminescence performed at UofSC. RL measurements performed at the Clemson University.

Appendix A. Supplementary data

Supplementary data to this article can be found online at https://doi.org/10.1016/j.solidstatesciences.2022.106861.

References

[1] E. Yoshida, Y. Hirano, H. Tashima, N. Inadama, F. Nishikido, T. Moriya, T. Omura, M. Watanabe, H. Murayama, T. Yamaya, The X'tal cube PET detector with a monolithic crystal processed by the 3D sub-surface laser engraving technique: performance comparison with glued crystal elements, Nucl. Instrum. Methods Phys. Res., Sect. A 723 (2013) 83–88.
[2] J. Tous, K. Blazek, L. Pina, B. Sopko, High-resolution imaging of biological and other objects with an X-ray digital camera, Appl. Radiat. Isot. 68 (2010) 651–653.
[3] H.I. West, W.E. Meyerhof, R. Hofstadter, Detection of X-rays by means of NaI(Tl) scintillation counters, Phys. Rev. 81 (1951) 141.
[4] B.K. Cha, J.-H. Shin, J.H. Bae, C.-h. Lee, S. Chang, H.K. Kim, C.K. Kim, G. Cho, Scintillation characteristics and imaging performance of CsI:Tl thin films for X-ray imaging applications, Instrum. Methods Phys. Res., Sect. A 604 (2009) 224–228.
[5] J. Glodo, W.M. Higgins, E.V.D. van Loef, K. Shah, Scintillation properties of 1 inch Cs_2LiYCl_6:Ce crystals, IEEE Trans. Nucl. Sci. 55 (2008) 1206–1209.
[6] B. Liu, C. Shi, M. Yin, Y. Fu, G. Zhang, G. Ren, Luminescence and energy transfer processes in $Lu_2SiO_5:Ce^{3+}$ scintillator, J. Lumin. 117 (2006) 129–134.
[7] M. Nikl, A. Yoshikawa, K. Kamada, K. Nejezchleb, C.R. Stanek, J.A. Mares, K. Blazek, Development of LuAG-based scintillator crystals - a review, Prog. Cryst. Growth Char. Mater. 59 (2013) 47–72.
[8] V.V. Laguta, M. Nikl, J. Rosa, B.V. Grinyov, L.L. Nagornaya, I.A. Tupitsina, Electron spin resonance study of self-trapped holes in $CdWO_4$ scintillator crystals, J. Appl. Phys. 104 (2008) 103525.
[9] K. Tagaki, T. Oi, T. Fukazawa, M. Ishii, S. Akiyama, Improvement in the scintillation conversion efficiency of $Bi_4Ge_3O_{12}$ single crystals, J. Cryst. Growth 52 (1981) 584–587.
[10] A.M. Latshaw, G. Morrison, K.D. zur Loye, A.R. Myers, M.D. Smith, H.-C. zur Loye, Intrinsic blue-white luminescence, luminescence color tunability, synthesis, structure, and polymorphism of $K_3YSi_2O_7$, CrystEngComm 18 (2016) 2294–2302.
[11] M. Bharathy, V.A. Rassolov, S. Park, H.-C. zur Loye, Crystal growth of two new photoluminescent oxides: $Sr_3Li_6Nb_2O_{11}$ and $Sr_3Li_6Ta_2O_{11}$, Inorg. Chem. 47 (2008) 9941–9945.
[12] I.P. Roof, T.-C. Jagau, W.G. Zeier, M.D. Smith, H.-C. zur Loye, Crystal growth of a new series of complex niobates, $LnKNaNbO_5$ (ln =La, Pr, Nd, Sm, Eu, Gd, and Tb): structural properties and photoluminescence, Chem. Mater. 21 (2009) 1955–1961.
[13] G.B. Ayer, M.D. Smith, L.G. Jacobsohn, G. Morrison, H.B. Tisdale, L.S. Breton, W. Zhang, P.S. Halasyamani, H.-C. zur Loye, Synthesis of hydrated ternary lanthanide-containing chlorides exhibiting X-ray scintillation and luminescence, Inorg. Chem. 60 (2021) 15371–15382.
[14] G. Morrison, A.M. Latshaw, N.R. Spagnuolo, H.-C. zur Loye, Observation of intense X-ray scintillation in a family of mixed anion silicates, $CsRESi_4O_{10}F_2$ (RE = Y, Eu-Lu), obtained viaan enhanced flux crystal growth technique, J. Am. Chem. Soc. 139 (2017) 14743–14748.
[15] G.B. Ayer, V.V. Klepov, M.D. Smith, M. Hu, Z. Yang, C.R. Martin, G. Morrison, H.-C. zur Loye, $BaWO_2F_4$: a mixed anion X-ray scintillator with excellent photoluminescence quantum efficiency, Dalton Trans 49 (2020) 10734–10739.
[16] G.B. Ayer, G. Morrison, M.D. Smith, L.G. Jacobsohn, H.-C. zur Loye, Luminescence and scintillation of $[Nb_2O_2F_9]^{3-}$ -Dimer-Containing oxide-fluorides: $Cs_{10}(Nb_2O_2F_9)_3F$, $Cs_{9.4}K_{0.6}(Nb_2O_2F_9)_3F$, and $Cs_{10}(Nb_2O_2F_9)_3Cl$, Inorg. Chem. 61 (2022) 3256–3262.
[17] L. Krause, R. Herbst-Irmer, G.M. Sheldrick, D. Stalke, Comparison of silver and molybdenum microfocus X-ray sources for single-crystal structure determination, J. Appl. Crystallogr. 48 (2015) 3–10.
[18] Bruker, APEX3, Saint$^+$, TWINABS, and Sadabs, Bruker, AXS Inc., Madison, Wisconsin, USA, 2015.
[19] O.V. Dolomanov, L.J. Bourhis, R.J. Gildea, J.A. Howard, H. Puschmann, OLEX2: a complete structure solution, refinement and analysis program, J. Appl. Crystallogr. 42 (2009) 334–341.
[20] G.M. Sheldrick, Crystal structure refinement with SHELXL, Acta Crystallogr. C: Struct. Chem. 71 (2015) 3–8.

[21] A.L. Spek, Structure validation in chemical crystallography, Acta Crystallogr. Sect. D Biol. Crystallogr. 65 (2009) 148–155.
[22] H.-M. Kao, K.-H. Lii, The first observation of heteronuclear two-bond *J*-coupling in the solid state: crystal structure and solid-state NMR spectroscopy of $Rb_4(NbO)_2(Si_8O_{21})$, Inorg. Chem. 41 (2002) 5644–5646.
[23] M.P. Crosnier, D. Guyomard, A. Verbaere, Y. Piffard, Synthesis and structure of a novel polysilicate $Cs_4(NbO)_2[Si_8O_{21}]$, Eur. J. Solid State Inorg. Chem. 27 (1990) 435–442.
[24] G. Blasse, G.J. Dirksen, Luminescence of siliconiobates, Eur. J. Solid State Inorg. Chem. 28 (1991) 425–429.